EUROPEAN
ACADEMIC
RESEARCH

Correlated adatom in graphene:
a mean field theory study with spin-flip interaction

H. O. FROTA
ANGSULA GHOSH
Department of Physics, Institute of Exact Sciences
Federal University of Amazonas, Brazil

Abstract

   The formation of the localized magnetic moments is studied in a single-layer graphene sheet due to the presence of a quantum dot in one of the sublattices of the graphene sheet. The strong on-site Coulomb interaction and the spin flip terms have been considered to calculate the conductance using the Landauer formalism. The bare splitting of the levels and the Coulomb interaction generate the multiple conductance peaks and are crucial in determining the boundary between the magnetic and the non-magnetic states. A strong chemical potential dependence of the above phase boundary and also the conductance values are evident.

Key words: graphene; Graphene, Adatoms, Conductance, Magnetic moment, Anderson model.

1. INTRODUCTION

A considerable amount of work has confirmed that the linear dispersion of the two-dimensional massless quasiparticles in graphene gives rise to unusual properties suitable for nanoscience and nanotechnological electronics. This two-dimensional allotrope of carbon with the sp^2 hybridization state is distributed in a hexagonal lattice formed by two interpenetrating triangular sublattices, A and B. Moreover, as a two-dimensional Dirac fermion system, it presents

an unconventional and interesting electronic behavior. For instance, a minimum conductivity of about e^2/h, an anomalous quantum Hall effect and a nonzero cyclotron mass m_c described by $E = m_c v_F^2$ are highly eminent.

Impurity states are regarded as important contributors to the unusual and singular properties of graphene. The effect of the impurities on the electronic and magnetic properties of single-layer pristine graphene has been widely dealt with in the context of spintronics. The magnetic moment formation is due to the presence of the transition-metal atoms envisions their application in spintronics and nanocatalysis. Moreover, magnetic impurities could envisage the creation of local spins in graphene including the possibility of opening a gap. Adatoms in graphene plays a special role as they can be tailored into graphene with atomic precision in order to create new many-body states that do not appear in pure graphene [1,2]. Furthermore, the electrical sensitivity to adatoms make its use viable as a single-molecule detector [3]. A systematic first-principles study of transition metals from Sc to Zn, including nonmagnetic adatoms Cu and Au, embedded in graphene has also been performed [4].

Magnetic adatom introduced in a metal has been successfully studied using the Anderson model [5,6], which recently has been applied also to study adatom in graphene [7,8,9,10]. Depending on the relation between the constitutive parameters of this model, the adatom orbital can be empty, single or doubly occupied. The electron-electron interaction in the adatoms within the mean-field scenario demonstrate a very different picture in graphene when compared to ordinary metals [7,8]. However, the above mean-field treatment fails to incorporate strong correlations in the adatoms. It is essential to consider calculations beyond mean-field to include the above correlations.

In the present work we study the formation of the local magnetic atoms due to the presence of adatoms in pristine graphene utilizing two approaches in the Green's function formalism. The first we consider the correlation without including the spin-flip terms whereas the second contemplates the spin-flip terms in the transport behavior.

2. THE MODEL

The model Hamiltonian of graphene with a strongly interacting impurity hybridized with a sublattice of graphene is written as

$$H = H_{TB} + H_f + H_V \qquad (1)$$

where H_{TB} is the tight binding Hamiltonian of the graphene, H_f is the impurity Hamiltonian and H_V is the hybridization of the adatom localized states with the graphene conduction electrons.

The tight binding Hamiltonian of graphene is given by

$$H_{TB} = -t \sum_{\langle i,j \rangle \sigma} \left[a_\sigma^\dagger(\mathbf{R}_i) b_\sigma(\mathbf{R}_j) + H.c. \right] \qquad (2)$$

where the operator $a_\sigma(\mathbf{R}_i)[b_\sigma(\mathbf{R}_j)]$ annihilates a state with spin σ at the position $\mathbf{R}_i(\mathbf{R}_j)$ on the sublattice A(B), $\langle i,j \rangle$ stands for summation over nearest neighbors and the parameter t is the nearest neighbor hopping energy. In momentum space, we have

$$H_{TB} = -t \sum_{\mathbf{k},\sigma} \left[\phi(\mathbf{k}) a_{\mathbf{k},\sigma}^\dagger b_{\mathbf{k},\sigma} + \phi^*(\mathbf{k}) b_{\mathbf{k},\sigma}^\dagger a_{\mathbf{k},\sigma} \right], \qquad (3)$$

where $\phi(\mathbf{k}) = \sum_\ell e^{i\mathbf{k}\cdot\boldsymbol{\delta}_\ell}$ ($\ell = 1,2,3$), with $\boldsymbol{\delta}_1 = a(\hat{\mathbf{x}}/2 + \sqrt{3}/2\hat{\mathbf{y}})$, $\boldsymbol{\delta}_2 = a(\hat{\mathbf{x}}/2 - \sqrt{3}/2\hat{\mathbf{y}})$ and $\boldsymbol{\delta}_3 = -a\hat{\mathbf{x}}$ are the nearest neighbor vectors, and a is the interatomic distance. Diagonalizing the Hamiltonian (3) one generates two bands $\varepsilon_\pm(\mathbf{k}) = \pm t|\phi(\mathbf{k})|$, which can be linearized around the Dirac points $\mathbf{K}$ at the corners of the Brillouin zone: $\varepsilon_\pm(\mathbf{K} + \mathbf{q}) \simeq \pm v_F |\mathbf{q}|$, where $v_F = 3ta/2$ is the Fermi velocity of the Dirac electrons. Hence the Hamiltonian H_{TB} can be written as

$$H_{TB} = \sum_{\mathbf{k},\sigma} \left[\varepsilon_+(\mathbf{k}) c_{\mathbf{k},\sigma}^\dagger c_{\mathbf{k},\sigma} + \varepsilon_-(\mathbf{k}) d_{\mathbf{k},\sigma}^\dagger d_{\mathbf{k},\sigma} \right]. \qquad (4)$$

The impurity Hamiltonian is described by

$$H_f = \sum_\sigma \varepsilon_{f\sigma} f_\sigma^\dagger f_\sigma + U n_\uparrow n_\downarrow, \qquad (5)$$

where $f_\sigma^\dagger$ is the creation operator of a state with a spin $\sigma = \uparrow, \downarrow$ of the impurity, $n_\sigma = f_\sigma^\dagger f_\sigma$ is the occupation number operator $\varepsilon_{f\sigma}$ is the

energy of the adatom electron, and U is the Coulomb interaction due to the double occupancy of an energy level in the adatom.

The hybridization of the impurity orbital with an atom of the subspace B of graphene is given by

$$H_V = \frac{1}{\sqrt{N_b}} \sum_{\mathbf{k},\sigma} V_{b\sigma} b_{\mathbf{k}\sigma}^{\dagger} f_{b\sigma} + H.c,$$
(6)

where N_b and $V_{b\sigma}$ denote the number of atoms in the sublattice B and the hybridization interaction between the adatom and that sublattice, respectively.

3. THE FORMALISM

The formation of a magnetic moment depends on the occupation of the two spin states of the impurities. The localized moment is formed when $n_\uparrow \neq n_\downarrow$. The self-consistent calculations of the density of states in the presence of the hybridization $V_{b\sigma}$ is performed for the determination of the occupation of the impurities. The occupation of the impurity level can be determined by

$$n_\sigma = \frac{1}{2\pi} \int_{-\infty}^{\mu} d\omega A_{f\sigma}(\omega) n_F(\omega),$$
(7)

where the spectral function is given by

$$A_{f\sigma}(\omega) = -2\Im G_{f\sigma}^R(\omega).$$
(8)

In order to probe the single-particle properties, it is essential to measure the tunneling of the electrons. The adimensional differential conductance can be calculated in terms of the spectral function which is given by

$$G/G_0 = \sum_\sigma \int d\omega A_{f\sigma}(\omega) \left[n_F(\omega) - n_F(\omega + eV) \right]$$
(9)

To calculate the conductance G and the magnetic moments, it is essential to calculate the spectral function $A_{f\sigma}(w)$ using the equation of motion technique in the Green function formalism. The single particle retarded Green function of the f electrons is $G_{f\sigma}^R(t) = -i\theta(t) \left\langle \left[f_\sigma^\dagger(t), f_\sigma(t) \right] \right\rangle$. Due to the strong interactions, it is essential to treat correlations properly as the motion of the

electrons hopping and, thereby, the current through the dot will be correlated, reason by which a mean-field approximation would becomes inappropriate. Hence, the iteration of the equation of motion generates two new terms [11]. Terms like

$$F^R((n_{f\bar{\sigma}}c_{\mathbf{k}\sigma})f_\sigma, t-t') = -i\theta(t-t')\langle[n_{f\bar{\sigma}}c_{\mathbf{k}\sigma}(t), f_\sigma(t')]\rangle \quad \text{and}$$

$$F^R((n_{f\bar{\sigma}}d_{\mathbf{k}\sigma})f_\sigma, t-t') = -i\theta(t-t')\langle[n_{f\bar{\sigma}}d_{\mathbf{k}\sigma}(t), f_\sigma(t')]\rangle \quad \text{appear, given}$$

rise to a new type of correlation, corresponding to a spin-flip term between the conduction and the adatom electrons. In the first moment, the intricate correlation functions will be neglected but in the second part of our calculation, we shall deal with these terms in detail. The Fourier transformed $G^R_{f\sigma}(\omega)$ has two resonances – one at $\varepsilon_{f\sigma}$, weighted by the probability $1-\langle n_{f\sigma}\rangle$, and the other at $\varepsilon_{f\sigma}+U$, weighted by the probability $\langle n_{f\sigma}\rangle$. Hence, we can write,

$$G^R_{f\sigma}(\omega) = \frac{1-\langle n_{f\bar{\sigma}}\rangle}{\omega-\grave{o}_{f\sigma}-\Sigma_0(\omega)} - \frac{\langle n_{f\bar{\sigma}}\rangle}{\omega-\grave{o}_{f\sigma}-U-\Sigma_0(\omega)} \quad , \qquad (10)$$

where

$$\Sigma_0(\omega) = -\frac{V^2_{b\sigma}}{2D^2}\left\{\omega \ln\left(\frac{|\omega^2-D^2|}{\omega^2}\right) + i\pi|\omega|\theta(D-|\omega|)\right\}, (11)$$

D is a high-energy cutoff of the order of the graphene bandwidth chosen according to the Debye prescription [7]. We assume also that $\mu \Box D$, where the band effects does not depend on the above cut-off. Remembering that the above calculations represent the tunneling of the σ electrons, neglecting the spin-flip contributions. In the following part of the section we calculate the conductance and the densities utilizing the spin-flip terms. It is important to note the following relations [12] before we proceed into our calculations.

$$\begin{aligned}
\langle c^\dagger_{k\sigma}f_\sigma\rangle &= 0 \\
\{f^\dagger_{\bar{\sigma}}(t)c_{k\bar{\sigma}}(t)c_{k'\sigma}(t), f^\dagger_\sigma(0)\} &= 0 \\
\{c^\dagger_{k\bar{\sigma}}(t)f_{\bar{\sigma}}(t)c_{k'\sigma}(t), f^\dagger_\sigma(0)\} &= 0 \\
\{c^\dagger_{k\bar{\sigma}}(t)c_{k'\bar{\sigma}}(t)f_\sigma(t), f^\dagger_\sigma(0)\} &= \delta_{k,k'}f_{FD}(\grave{o}_{k\bar{\sigma}})\times\{f_\sigma(t)f_\sigma(0)\}.
\end{aligned} \qquad (12)$$

Hence, considering the spin-flip terms, we can write $G^R_{f\sigma}(w)$ as

$$G_{f\sigma}^{R}(\omega) = \frac{1-\langle n_{f\bar{\sigma}}\rangle}{\omega-\dot{o}_{f\sigma}-\Sigma_0(\omega)-\dfrac{U\Sigma_2(\omega)}{(\omega)\big(\omega-\dot{o}_{f\sigma}-U-\Sigma_0(\omega)+\Sigma_1(\omega)\big)}}$$

$$+\frac{n_{f\bar{\sigma}}}{\left[\omega-\dot{o}_{f\sigma}-\Sigma_0(\omega)-\dfrac{U\Sigma_2(\omega)}{\omega-\dot{o}_{f\sigma}-U-\Sigma_0(\omega)+\Sigma_1(\omega)}\right]}$$

$$\times\frac{1}{\dfrac{\omega-\dot{o}_{f\sigma}-U-\Sigma_0(\omega)+\Sigma_1(\omega)}{\omega-\dot{o}_{f\sigma}-\Sigma_0(\omega)+\Sigma_1(\omega)}}. \tag{13}$$

The self energies Σ_α for $\alpha=1,2$, due to the tunneling of the electrons, can be written as

$$\Sigma_\alpha(\omega) = \frac{V_{b\bar{\sigma}}^2}{2N_B}\sum_k\left[\frac{A_{K\alpha}^{+}}{\omega-\dot{o}_{f\sigma}-\dot{o}_{f\bar{\sigma}}+\dot{o}_{+}(\mathbf{k})}+\frac{A_{K\alpha}^{-}}{\omega-\dot{o}_{f\sigma}-\dot{o}_{f\bar{\sigma}}+\dot{o}_{-}(\mathbf{k})}\right.$$
$$\left.-\frac{A_{K\alpha}^{+}}{\omega-\dot{o}_{f\sigma}+\dot{o}_{f\bar{\sigma}}-\dot{o}_{+}(\mathbf{k})}-\frac{A_{K\alpha}^{-}}{\omega-\dot{o}_{f\sigma}+\dot{o}_{f\bar{\sigma}}-\dot{o}_{-}(\mathbf{k})}\right], \tag{14}$$

where $A_{K1}^{+}=A_{K1}^{-}=1$ and $A_{K2}^{+}=f_{FD}(\varepsilon_{+}(\mathbf{k}))$ and $A_{K2}^{-}=f_{FD}(\varepsilon_{-}(\mathbf{k}))$.

The equation of motion solution of Eq. (10) and Eq. (13) for $G_{f\sigma}^{R}(\omega)$ are employed to calculate the magnetic moments and the conductance via the Landauer formula. We observe a chemical potential dependence of the magnetic regions and occupation in both the cases.

4. RESULTS AND DISCUSSION

In this section, we present densities and the conductance of the impurity coupled with B sublattice of the graphene layer. The dimensionless hybridizations for $\sigma=\uparrow,\downarrow$ are given by $\Gamma_\sigma=\pi V_\sigma^2/D^2$. For sake of numerical calculation, the graphene is represented by the bandwidth $D=7.0$ eV [7] and the interatomic spacing $a=0.14$ nm

[13]. It is important to note that all the parameters are written in terms of the bandwidth D, unless stated otherwise.

In Fig. (1) we exhibit the occupation n_σ as a function of chemical potential μ in units of D, for $U = 0.5$, $T = 0.01$, $\Gamma_\uparrow = \Gamma_\downarrow = 0.01$ and the following values of $\varepsilon_{f\uparrow}$ and $\varepsilon_{f\downarrow}$ respectively: (0.2, 0.2) (solid line), (0.2, 0.25) (dashed line), (0.2, 0.3) (dotted line). For $\varepsilon_{f\uparrow} = \varepsilon_{f\downarrow}$, no magnetic moments are formed and $n_\uparrow = n_\downarrow$. However, for $n_\uparrow \neq n_\downarrow$ we observe the prominent magnetic regions as seen in the figure. The magnetization is maximum in the bare level spacing $\Delta_\varepsilon = \varepsilon_{f\downarrow} - \varepsilon_{f\uparrow}$ firstly between $\varepsilon_{f\uparrow}$ and $\varepsilon_{f\downarrow}$ and thereafter between $\varepsilon_{f\uparrow} + U$ and $\varepsilon_{f\downarrow} + U$. The corresponding nature of the dimensionless conductance with μ for the same parameters as the above demonstrates two peaks for $\varepsilon_{f\uparrow} = \varepsilon_{f\downarrow}$ situated at $\varepsilon_{f\downarrow}$ and $\varepsilon_{f\downarrow} + U$. For $n_{f\uparrow} \neq n_{f\downarrow}$, we observe four peaks which depends on $\varepsilon_{f\uparrow}$, $\varepsilon_{f\downarrow}$ and U. As $\varepsilon_{f\downarrow}$ changes, the position of the first (third) peak at $\varepsilon_{f\uparrow}$ ($\varepsilon_{f\uparrow} + U$) remains unaltered, whereas the position of the second (fourth) peak suffers modification. The suppression of the peaks is discernible. The suppression of the peaks follows from the dependence of the DOS of each level on the occupancy of the other level. The dependencies on the spin-dependent couplings are studied in Fig. 3. As $\Gamma_\uparrow$ remains unchanged the conductance for $\sigma = \uparrow$ remains unaltered, whereas the increase in $\Gamma_\downarrow$ decreases and widens the conductance value. In Fig. 1(d), the temperature effect can be observed in the conductance values. The height of all the four peaks decreases with temperature as both the up-spin and the down-spin level are coupled in the same manner to graphene. The height of the first two peaks are $\Box 1/T$, whereas the second two peaks gets modified by the Coulomb interaction.

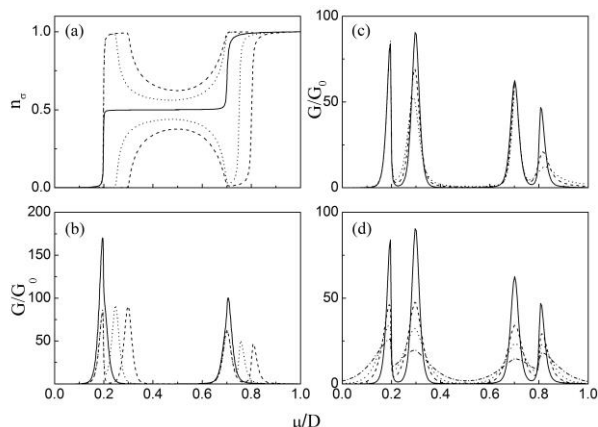**Figure 1:** (a) Occupation n_σ as a function of chemical potential μ in units of D, for $U=0.5$, $T=0.01$ $\Gamma_\uparrow = \Gamma_\downarrow = 0.01$ and the following values of $\varepsilon_{f\uparrow}$ and $\varepsilon_{f\downarrow}$ respectively: (0.2, 0.2) (solid line), (0.2, 0.25) (dashed line), (0.2, 0.3) (dotted line). Dimensionless conductance G/G_0 vs μ for (b) the same parameters as in (a), (c) $U=0.5$, $T=0.01$, $\varepsilon_{f\uparrow}=0.2$, $\varepsilon_{f\downarrow}=0.3$ and $\Gamma_\uparrow = \Gamma_\downarrow = 0.01$ (solid line), $\Gamma_\uparrow = 0.01$ and $\Gamma_\downarrow = 0.05$ (dashed line), $\Gamma_\uparrow = 0.01$ and $\Gamma_\downarrow = 0.1$ (dotted line) (d) $U=0.5$, $\varepsilon_{f\uparrow}=0.2$, $\varepsilon_{f\downarrow}=0.3$, $\Gamma_\uparrow = \Gamma_\downarrow = 0.01$ at $T=0.01$ (solid line), 0.02 (dashed line), 0.03 (dotted line), 0.05 (dashed-dotted line).

The conductance G/G_0 is plotted in Fig. (2) for $U=0.5$, $\Gamma_\uparrow = 0.01$, $\Gamma_\downarrow = 0.1$, $\varepsilon_{f\uparrow}=0.2$, $\varepsilon_{f\downarrow}=0.3$ at $T=0.01$ (solid line), 0.02 (dashed line), 0.05 (dotted line) and 0.06 (dashed-dotted line). Unlike the three peaks at $\varepsilon_{f\uparrow}$ and $\varepsilon_{f\uparrow}+U$ that decreases with T, the peak at $\varepsilon_{f\downarrow}+U$ increases with temperature after an initial decrease with T. At even higher temperatures, all the peaks fall because of the depletion of the amplitude of $n'_F(w)$. The increase at medium temperatures could be attributed to a stronger interaction between $\sigma = \downarrow$ electrons and graphene.
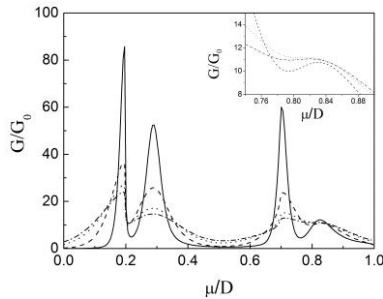
Figure 2: Conductance as a function of chemical potential in units of D, for $U = 0.5$, $\Gamma_\uparrow = 0.01$, $\Gamma_\downarrow = 0.1$, $\varepsilon_{f\uparrow} = 0.2$, $\varepsilon_{f\downarrow} = 0.3$ at $T = 0.01$ (solid line), 0.02 (dashed line), 0.05 (dotted line), 0.06 (dashed-dotted line).

The calculations of the occupation of the adatom atom as well as the dimensionless conductance taking into account the spin-flip terms are obtained from Eq. (13). The spin-flip terms not only modify the position of the peaks and the magnetic moments formation but also modifies to a great extent the dimensionless conductance values. In Fig. (3), the variation of the occupancy of the impurity electrons and the corresponding conductance are demonstrated with the change in $\varepsilon_{f\downarrow}$ in (a) and (c) and that with U in (b) and (d) respectively. We observe the shift in the peaks as we vary the two parameters and are in accord with our prior calculations.

Fig. (4) shows the relative change in the value of the four peaks owes it to the spin-flip terms where both $\Gamma_\uparrow$ and $\Gamma_\downarrow$ plays a considerable role unlike Fig. (1), where the spin-flip terms were ignored. Moreover, the width of the peaks also change as they are proportional to Γ_σ.
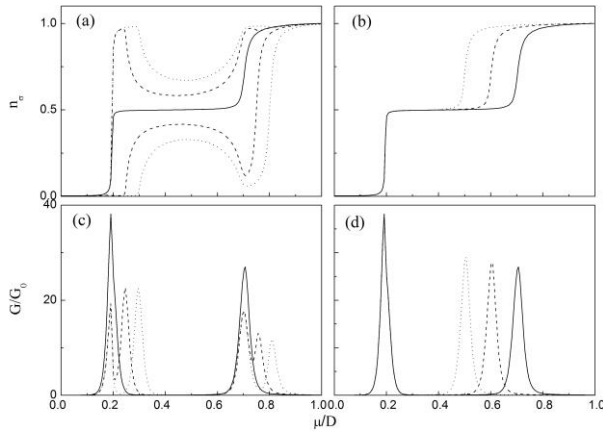
Figure 3: Occupation n_σ as a function of chemical potential μ in units of D, for $T = 0.01 \ \Gamma_\uparrow = \Gamma_\downarrow = 0.01$. (a) $U = 0.5$, and the following values of $\varepsilon_{f\uparrow}$ and $\varepsilon_{f\downarrow}$ respectively: (0.2, 0.2) (solid line), (0.2, 0.25) (dashed line), (0.2, 0.3) (dotted line); (b) $\varepsilon_{f\uparrow} = \varepsilon_{f\downarrow} = 0.2$, $U = 0.3$ (solid line), $U = 0.4$ (dashed line) and $U = 0.5$ (dotted line); (c) dimensionless conductance G/G_0 versus μ for the same parameters as in (a); (d) dimensionless conductance G/G_0 versus μ and for the same parameters as in (b).
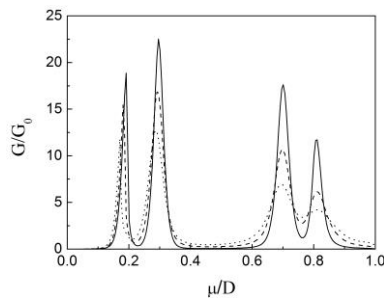

Figure 4: Dimensionless conductance G/G_0 versus μ for $U = 0.5$, $T = 0.01$, $\varepsilon_{f\uparrow} = 0.2$, $\varepsilon_{f\downarrow} = 0.3$ and $\Gamma_\uparrow = \Gamma_\downarrow = 0.01$ (solid line), $\Gamma_\uparrow = 0.01$ and $\Gamma_\downarrow = 0.05$ (dashed line), $\Gamma_\uparrow = 0.01 \ \Gamma_\downarrow = 0.1$ (dotted line).

The temperature dependencies of the conductance values are demonstrated in Fig. (5). The considered values of the parameters are $\Gamma_\uparrow = 0.01$, $\Gamma_\downarrow = 0.1$, $\varepsilon_{f\uparrow} = 0.2$, $\varepsilon_{f\downarrow} = 0.3$ at $T = 0.01$ (solid line), 0.02 (dashed line), 0.03 (dotted line), 0.05 (dashed-dotted line) and 0.07 (dashed-double-dotted line). The height of the peaks decreases substantially with the increase in temperature. The increase in the relative distance between the third and the fourth peaks compared to that of Fig. (2) eliminates the anomalous nature of the fourth peak. Thus the temperature tends to decrease the conductance values with the increase in temperature.
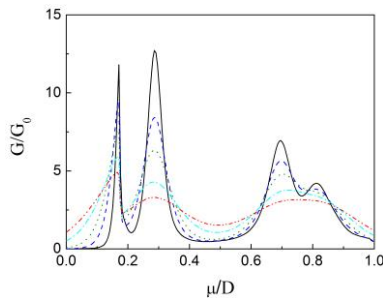

Figure 5: Conductance as a function of chemical potential in units of D, for U=0.5, G_-=0.01,G_-=0.1, e_{f-}=0.2,e_f=0.3 at T=0.01 (solid line), 0.02 (dashed line), 0.03 (dotted line), 0.05 (dashed-dotted line) and 0.06 (dashed-double-dotted line)

5. CONCLUSION

In summary, we study the effect of the strong on-site interaction of the quantum-dot interacting with a sublattice of single-layer graphene. The correlation effects on the conductance values have been considered through a iterative process in an Anderson model. The presence of the four peaks in the conductance peaks could be explained in terms of the bare-energy-level spacing and the strong Coulomb-interaction energy. The temperature dependencies of the conductance peaks demonstrates an overall decreases in its value. The height of the conductance peaks also decrease with the inclusion of the spin-flip terms.

Acknowledgment

The authors acknowledge financial support from the Brazilian funding agencies CNPq and CAPES.

Declaration of competing interest

The authors declare that they have no known competing financial interests or personal relationships that could have appeared to influence the work reported in this paper.

Credit authorship contribution statement

H. Frota: Conceptualization, Methodology, Analysis, Writing - review & editing, Funding acquisition. A. Ghosh: Calculations, Numerical calculations, Analysis, Writing - original draft, Funding acquisition

REFERENCES

[1] Uchoa, B, Lin, C.-Y. & Castro Neto, A.H.. (2008). Tailoring graphene with metals on top. *Phys. Rev. B*, 77, 035420-5.

[2] Eigler, D. M. & Schweizer, E. K. (1990). Positioning single atoms with a scanning tunnelling microscope. *Nature*, 344, 524-526.

[3] Schedin, F., Geim, A. K., Morozov, S. V., Hill, E. W., Blake, P., Katsnelson, M. I. & Novoselov, K. S. . (2007). Detection of individual gas molecules adsorbed on graphene. *Nature Materials*, 6, 652-655.

[4] Krasheninnikov, A. V. , Lehtinen, P. O., Foster, A. S., Pyykkö, P. & R. M. Nieminen. (2009). Embedding Transition-Metal Atoms in Graphene: Structure, Bonding, and Magnetism. *Phys. Rev. Lett.*, 102, 126807-4.

[5] Anderson, P. W. . (1961). Localized Magnetic States in Metals. *Phys. Rev.*, 124, 41-53.

[6] Alexander, S. & Anderson, P. W.. (1964). Interaction Between Localized States in Metals. *Phys. Rev.*, 133, A1594-1603.

[7] Uchoa, B., Kotov, V. N., Peres, N. M. R. & Castro Neto, A. H.. (2008). Localized Magnetic States in Graphene. *Phys Rev. Lett.* 101, 026805-4.

[8] Ghosh, A. & Frota, H. O. (2012). NMR of localized magnetic states in graphene. *Physica B,* 407, 1170-1174.

[9] Hu, F. M. , Kou, L & Frauenheim, T.. (2015). Controllable magnetic correlation between two impurities by spin-orbit coupling in graphene. *Scientific Rep*., 5, 8943-5.

[10] Castro Neto, A.H. , Kotov, V.N., Nilsson, J., Pereira, V.M., Peres, N.M.R. & Uchoa, B.. (2009). Adatoms in graphene. *Solid State Communications* , 149, 1094-1100.

[11] Bruus, H. & Flensberg, K.. (2004). *Many Body Quantum theory in condensed matter physics*. Oxford: Oxford Graduate texts.

[12] Meir, Y., Wingreen, N. S. & P. A. Lee. (1991). Transport through a strongly interacting electron system: Theory of periodic conductance oscillations. *Phys, Rev. Lett*., 66, 3048-3051.

[13] Das Sarma, S., Adam, S., Hwang, E. H. & Rossi, E..(2011). Electronic transport in two-dimensional graphene. *Rev. Mod. Phys.*, 83, 407-470.